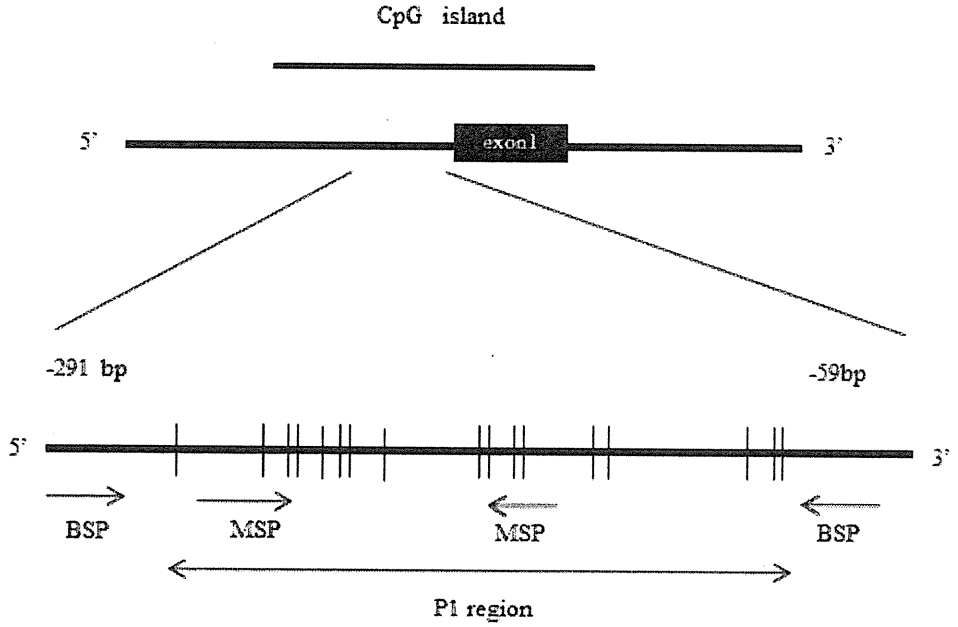

Figure 1

A

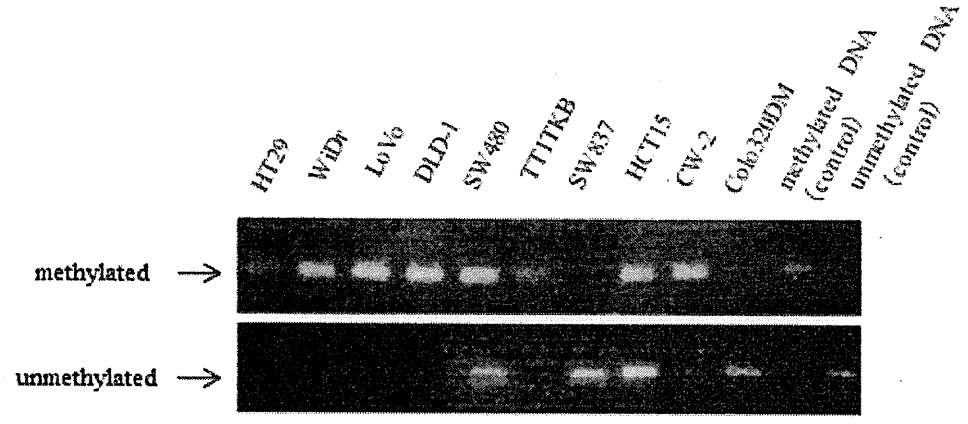
HT29
WiDr
LoVo
DLD-1
SW480
TT1TKB
SW837
HCT15
CW-2
Colo320DM
methylated DNA (control)
unmethylated DNA (control)
methylated
unmethylated

B

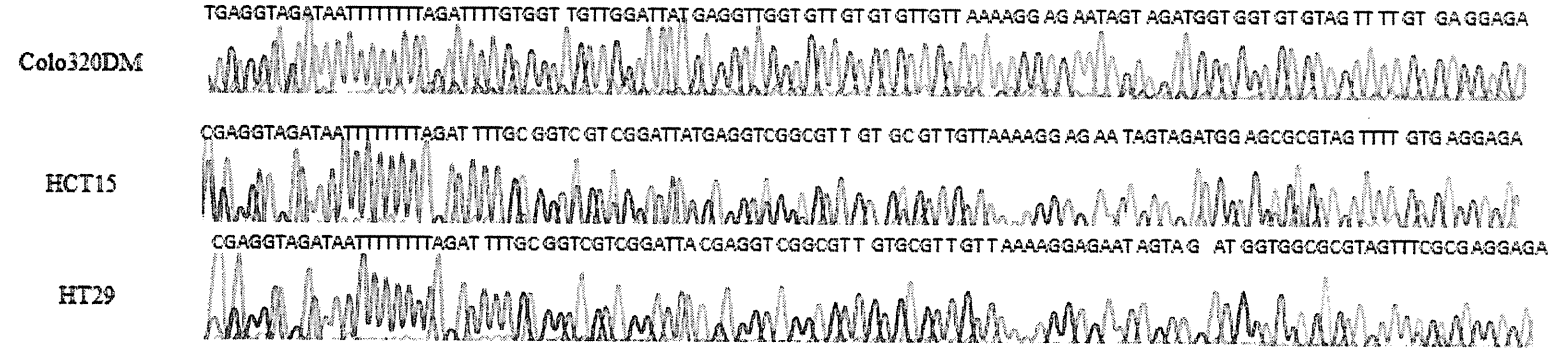
Colo320DM
TGAGGTAGATAATTTTTTTTAGATTTTGTGGT TGTTGGATTAT GAGGTTGGT GTT GT GT GTTGTT AAAAGG AG AATAGT AGATGGT GGT GT GTAG TT TT GT GA GGAGA
HCT15
CGAGGTAGATAATTTTTTTTAGAT TTTGC GGTC GT CGGATTATGAGGTCGGCGT T GT GC GT TGTTAAAAGG AG AA TAGTAGATGG AGCGCGTAG TTTT GTG AGGAGA
HT29
CGAGGTAGATAATTTTTTTTAGAT TTTGC GGTCGTCGGATTA CGAGGT CGGCGT T GTGCGT T GT T AAAAGGAGAAT AGTA G AT GGTGGCGCGTAGTTTCGCG AGGAGA

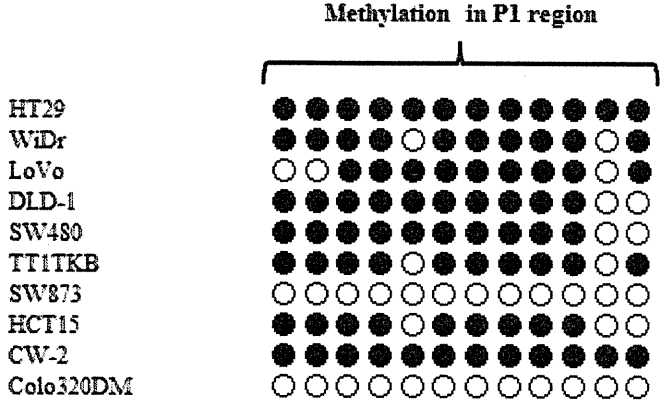
Methylation in P1 region
HT29
WiDr
LoVo
DLD-1
SW480
TT1TKB
SW873
HCT15
CW-2
Colo320DM

Figure 2

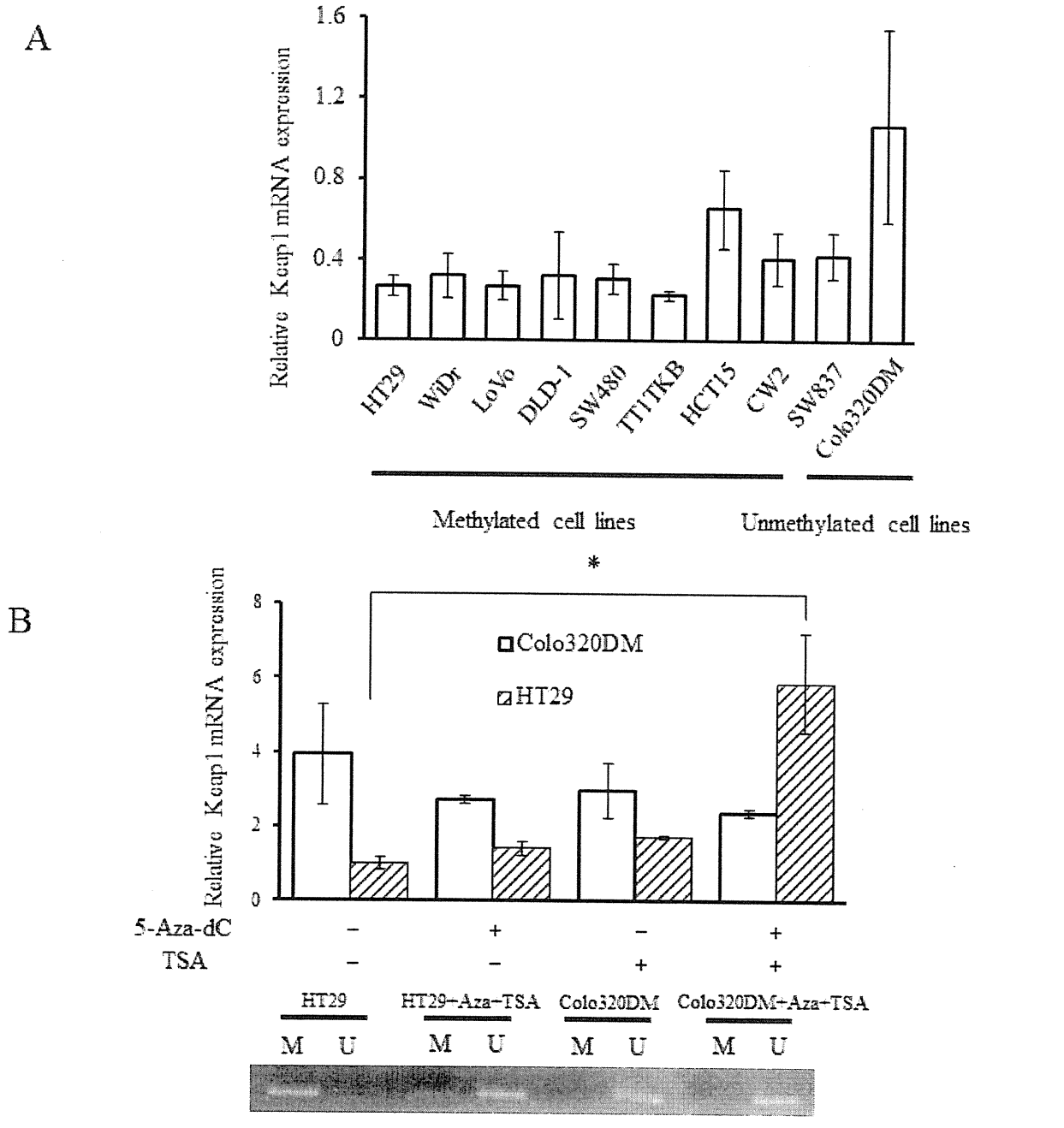
A
Relative Keap1 mRNA expression
1.6
1.2
0.8
0.4
0
HT29
WiDr
LoVo
DLD-1
SW480
TT1TKB
HCT15
CW2
SW837
Colo320DM
Methylated cell lines
Unmethylated cell lines
B
*
Relative Keap1 mRNA expression
8
6
4
2
0
Colo320DM
HT29
5-Aza-dC
TSA
HT29
HT29+Aza+TSA
Colo320DM
Colo320DM+Aza+TSA
M U M U M U M U
C
Colo320DM (W)
HT29 (W)
Keap1
65kD
β-actin
Colo320DM (C)
HT29 (C)
Colo320DM (N)
HT29 (N)
Nrf2
100kD
Histone H1
GAPDH

Figure 3

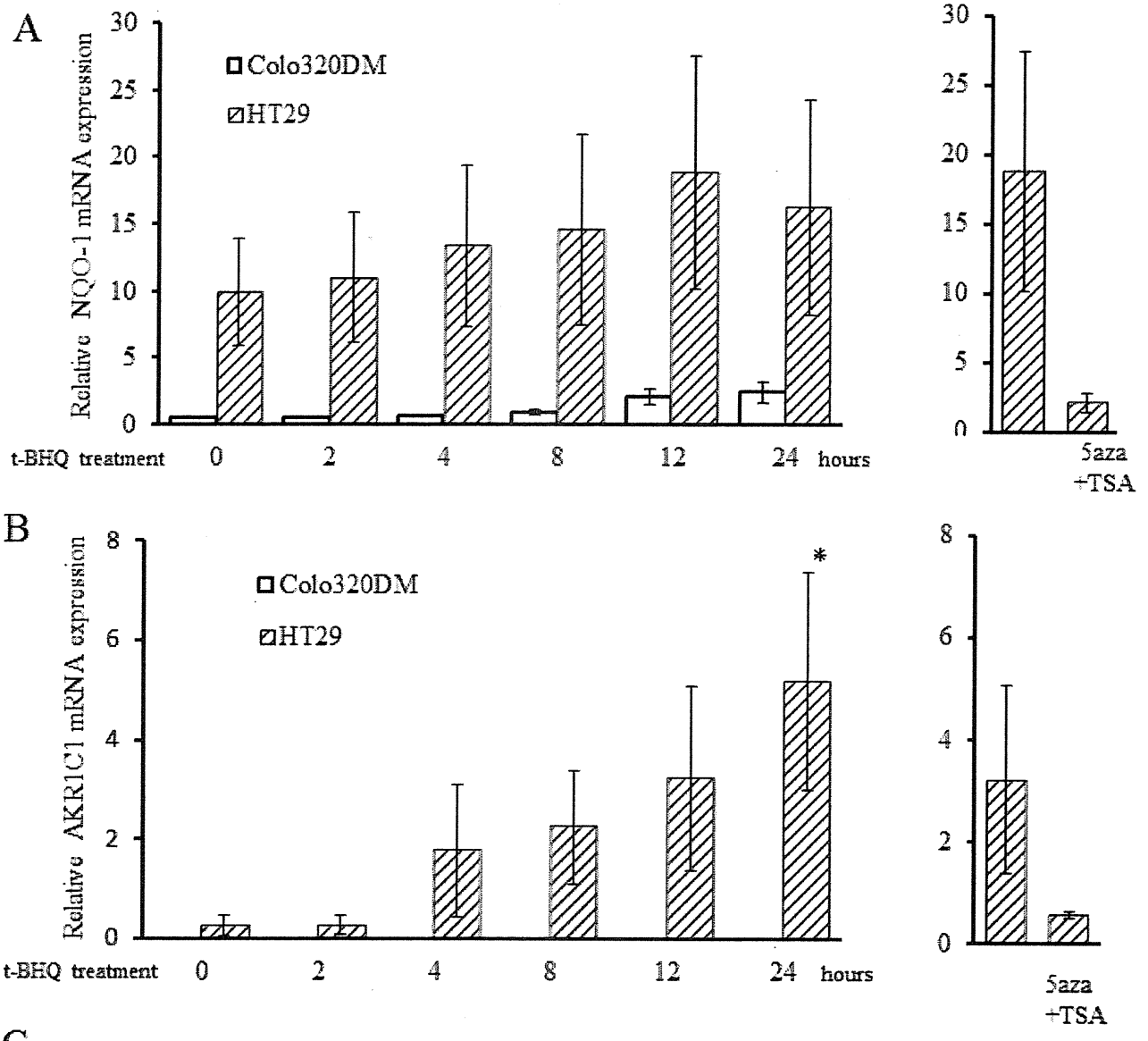
A
Relative NQO-1 mRNA expression
Colo320DM
HT29
t-BHQ treatment
0
2
4
8
12
24
hours
5aza
+TSA
B
Relative AKR1C1 mRNA expression
Colo320DM
HT29
*
t-BHQ treatment
0
2
4
8
12
24
hours
5aza
+TSA

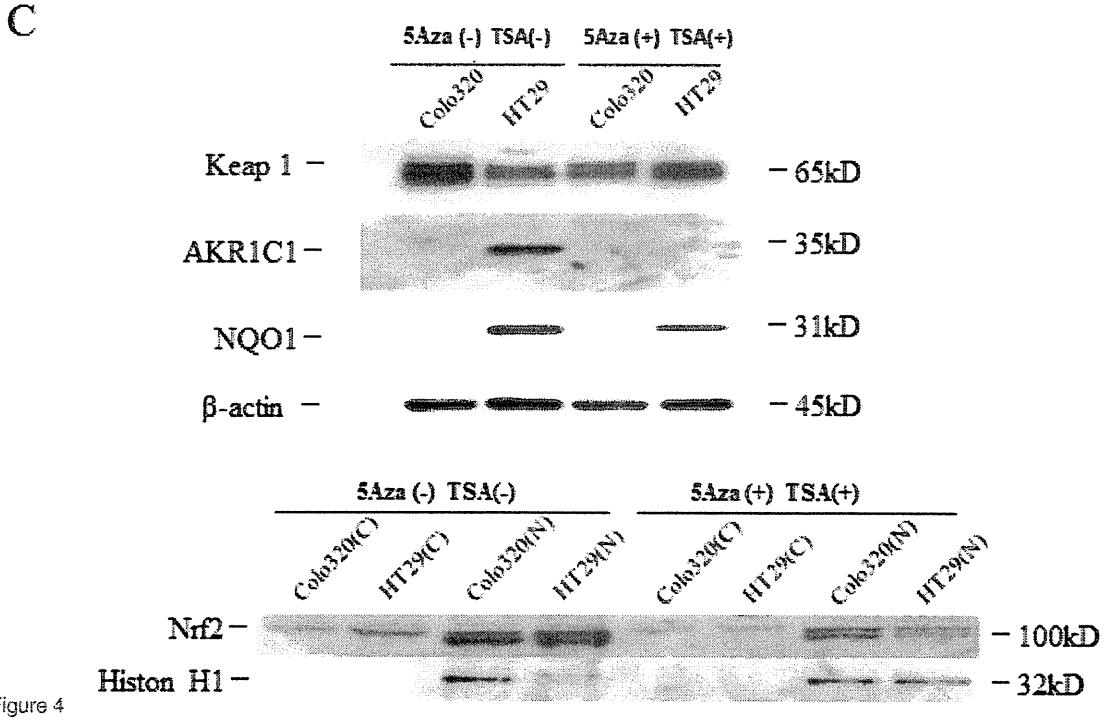
C
5Aza (-) TSA(-)
5Aza (+) TSA(+)
Colo320
HT29
Colo320
HT29
Keap 1
65kD
AKR1C1
35kD
NQO1
31kD
β-actin
45kD
5Aza (-) TSA(-)
5Aza (+) TSA(+)
Colo320(C)
HT29(C)
Colo320(N)
HT29(N)
Colo320(C)
HT29(C)
Colo320(N)
HT29(N)
Nrf2
100kD
Histon H1
32kD

Figure 4

A

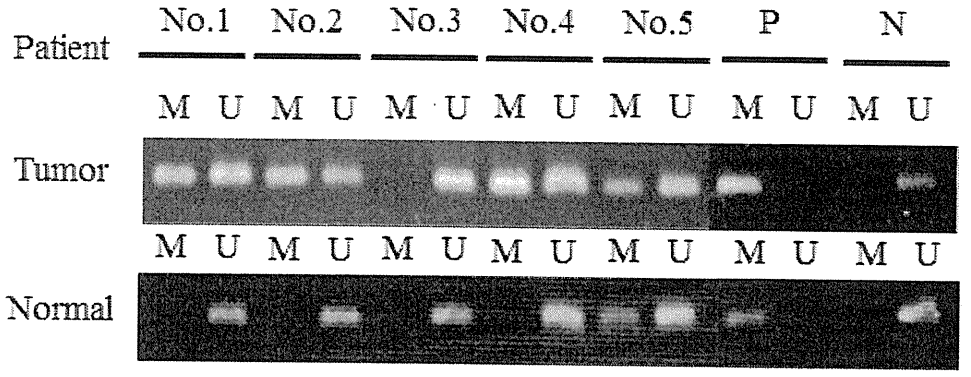
Patient
No.1 No.2 No.3 No.4 No.5 P N
M U M U M U M U M U M U M U
Tumor
M U M U M U M U M U M U M U
Normal

B

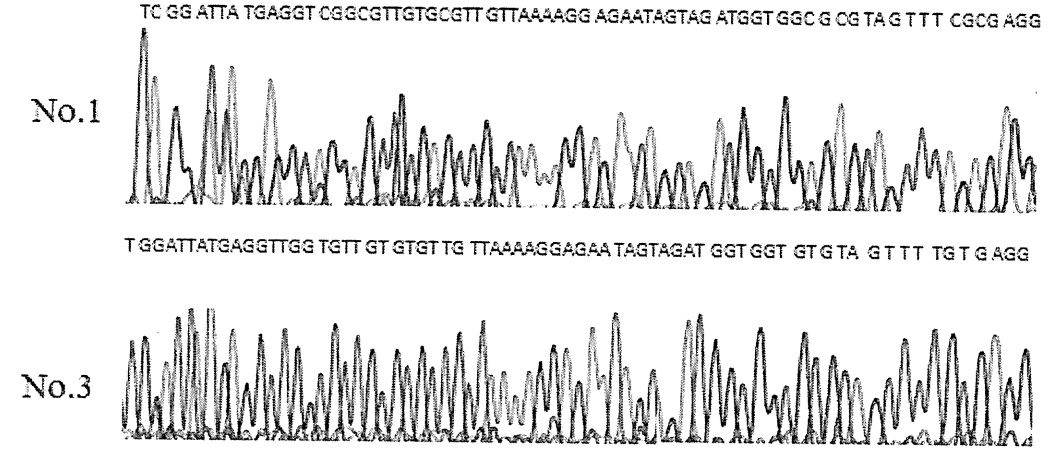
TC GG ATTA TGAGGT CGGCGTTGTGCGTT GTTAAAAGG AGAATAGTAG ATGGT GGC G CG TA G T T T CGCG AGG
No.1
T GGATTATGAGGTTGG TGTT GT GTGT TG TTAAAAGGAGAA TAGTAGAT GGT GGT GT G TA GT T T TG T G AGG
No.3

C

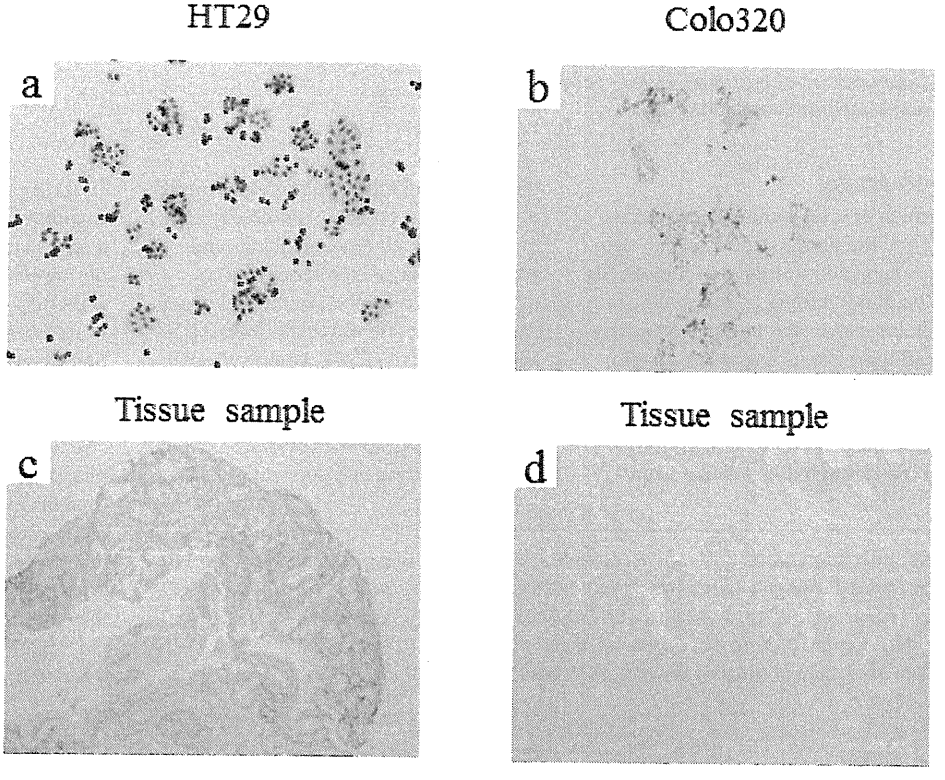
HT29
Colo320
a
b
Tissue sample
Tissue sample
c
d

Figure 5

Mesenchymal Stromal Cells Promote Tumor Growth through the Enhancement of Neovascularization

Kazuhiro Suzuki,[1,2] Ruowen Sun,[1,3] Makoto Origuchi,[4] Masahiko Kanehira,[4] Takenori Takahata,[1] Jugoh Itoh,[1] Akihiro Umezawa,[5] Hiroshi Kijima,[6] Shinsaku Fukuda,[2] and Yasuo Saijo[1]

[1]Department of Medical Oncology, Hirosaki University Graduate School of Medicine, Hirosaki, Japan; the [2]Department of Gastroenterology and Hematology, Hirosaki University Graduate School of Medicine, Hirosaki, Japan; the [3]Department of Rheumatology and Immunology, Shengjing Hospital of China Medical University, Shenyang, China; the [4]Department of Molecular Medicine, Tohoku University Graduate School of Medicine, Sendai, Japan; the [5]Department of Reproductive Biology, National Institute for Child Health and Development, Tokyo, Japan; and the [6]Department of Pathology and Bioscience, Hirosaki University Graduate School of Medicine, Hirosaki, Japan

Mesenchymal stromal cells (MSCs), also called mesenchymal stem cells, migrate and function as stromal cells in tumor tissues. The effects of MSCs on tumor growth are controversial. In this study, we showed that MSCs increase proliferation of tumor cells *in vitro* and promote tumor growth *in vivo*. We also further analyzed the mechanisms that underlie these effects. For use in *in vitro* and *in vivo* experiments, we established a bone marrow–derived mesenchymal stromal cell line from cells isolated in C57BL/6 mice. Effects of murine MSCs on tumor cell proliferation *in vitro* were analyzed in a coculture model with B16-LacZ cells. Both coculture with MSCs and treatment with MSC-conditioned media led to enhanced growth of B16-LacZ cells, although the magnitude of growth stimulation in cocultured cells was greater than that of cells treated with conditioned media. Co-injection of B16-LacZ cells and MSCs into syngeneic mice led to increased tumor size compared with injection of B16-LacZ cells alone. Identical experiments using Lewis lung carcinoma (LLC) cells instead of B16-LacZ cells yielded similar results. Consistent with a role for neovascularization in MSC-mediated tumor growth, tumor vessel area was greater in tumors resulting from co-injection of B16-LacZ cells or LLCs with MSCs than in tumors induced by injection of cancer cells alone. Co-injected MSCs directly supported the tumor vasculature by localizing close to vascular walls and by expressing an endothelial marker. Furthermore, secretion of leukemia inhibitory factor, macrophage colony-stimulating factor, macrophage inflammatory protein-2 and vascular endothelial growth factor was increased in cocultures of MSCs and B16-LacZ cells compared with B16-LacZ cells alone. Together, these results indicate that MSCs promote tumor growth both *in vitro* and *in vivo* and suggest that tumor promotion *in vivo* may be attributable in part to enhanced angiogenesis.

Online address: http://www.molmed.org
doi: 10.2119/molmed.2010.00157

INTRODUCTION

Growth of solid tumors requires formation of the tumor stroma, which supplies oxygen and nutrients to tumor cells (1). The tumor stroma is composed of extracellular matrix and various mesenchymal cell types, including macrophages, endothelial cells, lymphocytes, pericytes, fibroblasts and myofibroblasts (2). These stromal cells communicate with tumor cells both through direct contact and through paracrine signaling mechanisms, mediated by secretion of soluble factors, including cytokines, chemokines and growth factors (3–7). Interactions between tumor cells and stromal cells regulate tumor growth, invasion, metastasis and angiogenesis (3–7). Among stromal cells, tumor-associated fibroblasts have been shown to be associated with increases in tumor growth and metastatic potential, leading to a poor prognosis (8,9). Tumor-associated fibroblasts and myofibroblasts originate from multiple sources and range from migratory neighboring cells to distant invading cells (10). Data from human tumors and mouse tumor models suggest that at least a portion of the stromal cells are derived from the bone marrow (11–13).

Mesenchymal stromal cells (MSCs), also called mesenchymal stem cells, are pluripotent progenitor cells that have the capability to differentiate into chondrocytes, adipocytes and osteoblasts, among other types of cells (14). Although MSCs primarily reside in the bone marrow (15), they are also found in adipose tissue, in the lungs and in many other organs, where they are involved in maintenance

Address correspondence and reprint requests to *Yasuo Saijo, Department of Medical Oncology, Hirosaki University Graduate School of Medicine, 5 Zaifumacho, Hirosaki 036-8562, Japan. Phone: +81-172-39-5345; Fax: +81-172-39-5347; E-mail: yasosj@cc.hirosaki-u.ac.jp.*
Submitted August 20, 2010; Accepted for publication March 10, 2011; Epub (www.molmed.org) ahead of print March 11, 2011.

and regeneration of connective tissues (16). MSCs are known to migrate to tissues as a result of inflammation or injury, where they contribute to regeneration of the damaged tissues (17). For these reasons, MSCs have considerable therapeutic potential in tissue regeneration (18,19).

Recent results from both animal models and human tumors have suggested that MSCs also migrate to tumor tissues, where they incorporate into the tumor stroma (20,21). This tropism of MSCs for tumors is reportedly due to the presence of soluble factors secreted by tumor cells, similar to inflammatory responses (22,23). These findings have led to increased interest in understanding the effects of MSCs in the tumor microenvironment. Several studies have suggested that MSCs promote tumor growth and the metastatic potential of tumor cells (3,24). MSCs can differentiate into fibroblasts, myofibroblasts or pericyte-like cells and induce neoangiogenesis, resulting in the promotion of tumor growth *in vivo* (24,25). In contrast, few studies have indicated that MSCs inhibit tumor growth (26). Several studies have used human MSCs, as opposed to murine MSCs, to assess the effects of this cell type on tumor growth in mouse models because of the ease of expansion of human MSCs (3,24). In these tumor xenograft models, the tumor stroma consists of mouse cells, but the tumoral cells and MSCs are of human origin. Thus, because of the mixed lineages of these cells, the effects of MSCs on tumor growth may be affected by unknown interactions. On the basis of these previous studies, we elected to use only murine cells throughout the present study for the purpose of clearly interpreting the resulting findings.

In this study, we developed a quantitative assay for tumor growth *in vitro* using coculture models with MSCs and B16 melanoma cells expressing LacZ (B16-LacZ). We demonstrated that both direct contact with MSCs and release of soluble factors from MSCs promote B16-LacZ cancer cell proliferation *in vitro*. Furthermore, our results suggest that co-injection of MSCs with B16-LacZ cells promotes tumor formation in mice through enhanced angiogenesis, induced by secretion of proangiogenic factors from MSCs.

MATERIALS AND METHODS

Cell Culture and Animals

B16-LacZ, a mouse melanoma cell line expressing β-galactosidase, and TSt-4, a mouse MSC cell line derived from fetal thymus tissue (27), were obtained from the RIKEN BioResource Center (Tsukuba, Japan). B16-LacZ cells were cultured in Dulbecco's modified Eagle's medium (DMEM) supplemented with 10% fetal bovine serum (FBS; DMEM/10% FBS). Lewis lung carcinoma (LLC) cells were obtained from the Cell Resource Center for Biomedical Research, Tohoku University (Sendai, Japan). LLC cells were propagated in RPMI-1640 containing 10% FBS. A mouse bone marrow–derived mesenchymal cell line (MSC) was established from bone marrow cells isolated from C57BL/6 mice, as described previously (28). MSCs were cultured in DMEM low glucose 1× medium (DMEM + GlutaMAX; Invitrogen, San Diego, CA, USA) containing 10% FBS (Invitrogen). Female C57BL/6 mice, 6–8 wks of age, were purchased from Japan Charles River (Atsugi, Japan). Female C57BL/6-Tg (CAG-EGFP) Q1 mice were purchased from Japan SLC (Hamamatsu, Japan). For primary culture of MSCs from GFPQ2 mice, the bone marrow suspension was cultured in DMEM + GlutaMAX with 10% FBS. When adherent cells reached 70–80% confluence, cells were harvested and expanded. When a homogeneous cell population was obtained, after 3 to 5 passages, these cells were used for subsequent experiments.

Analysis of MSC Cell Surface Markers

Cell surface antigens were analyzed by flow cytometry in cultured murine MSCs. Briefly, 1×10^5 cells were incubated with the following fluorescence-conjugated rat monoclonal antibodies: antimouse Sca-1 (Ly-6A/E; BD Pharmingen, San Diego, CA, USA), antimouse CD44 (Pgp-1/Ly-24; eBioscience, San Diego, CA, USA), antimouse CD34 (Beckman Coulter, Fullerton, CA, USA), antimouse CD45 Q6 (leukocyte common antigen) (Beckman Coulter) and antimouse CD90 (Thy-1; Beckman Coulter). Nonspecific fluorescence was assessed by incubation of cells with isotype-matched rat monoclonal antibodies (BD Pharmingen). Data were analyzed by collecting 20,000 events on a Cell Lab Quanta SC (Beckman Coulter).

In Vitro Cell Proliferation Assays

For proliferation assays using cocultured cells, MSCs were seeded at 5.0×10^3 cells/well in 96-well plates in DMEM containing 1% FBS (DMEM/1% FBS). After 12 h, B16-LacZ cells were added (5.0×10^3 cells/well) to cultured MSCs. After an additional 24 h, cells were fixed by incubation in phosphate-buffered saline (PBS) containing 5.4% formaldehyde and 0.8% glutaraldehyde at 12-h time points. After two washes with PBS, 100 μL 5-bromo-4-chloro-3-indolyl-β-D-galactopyranoside (X-Gal) solution (2 mg/mL) was added to each well. Cells were then incubated at 37°C in a humidified atmosphere containing 5% CO_2 in the dark for 12 h. Absorbance at 595 nm was measured using an E-Max precision microplate reader (Molecular Devices, Menlo Park, CA, USA).

For proliferation assays performed in the absence of direct contact between MSCs and B16-LacZ cells, MSCs were seeded at a density of 5.0×10^4 cells/well in 24-well plates in DMEM/1% FBS. After a 12-h incubation, wells were covered with Cell Disks (Sumitomo Bakelite, Tokyo, Japan) that serve as a bulkhead, and B16-LacZ cells (5.0×10^4 cells/well) were added to the cell disks. After an additional 48 h, cells were lysed by the addition of lysis buffer (0.5% Triton X-100, 2 mol/L NaCl in PBS) at 12-h time points, and 100 μL 2 mg/mL X-Gal solution was combined with 15 μL of the cell suspension. The absorbance at 595 nm of the resulting solution was then measured as described above.

To assess cell proliferation in the presence of conditioned media from MSCs, media were collected from MSCs (2×10^6 cells) cultured in 10 mL DMEM/1% FBS in a culture dish (10 cm in diameter) for 48 h. The media were clarified by centrifugation (1,000*g*, 5 min), and the resulting supernatant was used as conditioned media. B16-LacZ cells were seeded at a density of 5.0×10^3 cells/well in 96-well plates and cultured in DMEM/10% FBS for 12 h. Subsequently, the media were replaced with either conditioned media or DMEM/1% FBS. Next, 10 μL Alamar Blue assay solution (Biosource International, Camarillo, CA, USA) was added to the wells at 12-h time points, and the plates were incubated at 37°C. Fluorescence was measured using a Fluoroskan Ascent CF apparatus (Labsystems, Helsinki, Finland) with excitation set to 544 nm and emission set to 590 nm.

Analysis of *In Vivo* Tumor Growth

All animal experiments were reviewed and approved by the Institutional Animal Care and Use Committee of Hirosaki University.

All mice (n = 8 for each group) were divided into groups that received subcutaneous injections of either (a) B16-LacZ cells alone (5.0×10^5 cells), (b) B16-LacZ cells (5.0×10^5 cells) with MSCs (1×10^5 cells) at a 1:0.2 ratio, (c) B16-LacZ cells (5.0×10^5 cells) with MSCs (5.0×10^5 cells) at a 1:1 ratio, (d) B16-LacZ (5.0×10^5 cells) with MSCs (2.5×10^6 cells) at a 1:5 ratio or (e) MSCs alone (2.5×10^6 cells). All cell suspensions were delivered in a final volume of 200 μL and injected subcutaneously into the right side of the abdomen. LLC cells were transplanted instead of B16-LacZ cells under identical conditions. Beginning 5 d after cell injections, the tumor volume was calculated every 2 d using the following formula: tumor volume (mm^3) = 0.52 × width $(mm)^2$ × length (mm).

Immunohistochemistry of the Tumors

B16-LacZ tumors on day 21 were removed, fixed in 10% buffered formalin for 24 h and then stained with hematoxylin and eosin for histological examination. For immunohistochemical staining for Ki-67, sections were deparaffinized and antigen retrieval was conducted using an antigen retrieval solution (415211; Nichirei, Tokyo Japan). After blocking of endogenous peroxidase activity with a peroxidase blocking reagent (S2001; Dako, San Antonio, TX, USA), tissue sections were incubated with rat antimouse Ki-67 (1:25; Dako) and the appropriate secondary antibody. Color development was performed using the peroxidase substrate 3-amino-9-ethylcarbazole.

To characterize the effects of MSCs on microvessel area in tumor tissues, tumors were removed when the tumor size reached around 1 cm^3 or at day 21. Cryosections were fixed with 4% paraformaldehyde and stained with rat antimouse CD31 (1:100; BD Pharmingen). Sections were then incubated with labeled polymer (N-Histofine Simple Stain Mouse MAX PO [Rat]; Nichirei, Tokyo, Japan). Color development was performed using 3-amino-9-ethylcarbazole. Sections were counterstained with hematoxylin. Microvessel area in cryosections from each tumor was quantified using 10 images from each of 10 different tumors per group under 200× magnification. Vessel area was measured using the ImageJ software (http://rsbweb.nih.gov/ij).

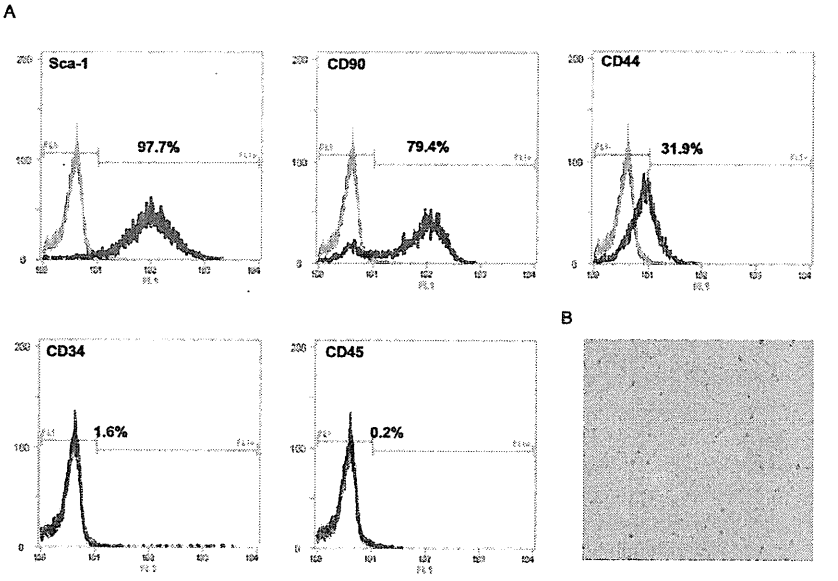

Figure 1. Flow cytometric and morphological analysis of MSCs. (A) Mouse bone marrow–derived MSCs established from cells obtained in C57BL/6 mice were stained with antibodies directed against Sca-1, CD90, CD44, CD34 and CD45 and were analyzed by flow cytometry. (B) Morphology of MSCs in culture.Q8

Immunofluorescence

On day 21, B16-LacZ tumors with MSCs expressing GFP (GFP-MSCs) were fixed with 4% paraformaldehyde and increasing concentrations of sucrose buffer (12%, 15% and 18%) over 12 h. Frozen sections were blocked with Protein Block Serum-Free (X0909; Dako) and were incubated with rat antimouse CD31 (1:100; BD Pharmingen) or rabbit antimouse α smooth muscle actin (α-SMA, 1:50, ab5694; Abcam, Cambridge, U.K.). Rat IgG_{2a} and rabbit IgG were used as isotype controls. Secondary antibodies used were donkey antirat IgG-Alexa Fluor 594 (1:200; Invitrogen) or goat antirabbit IgG-Alexa Fluor 594 (1:200; Invitrogen), respectively. To improve primary antibody penetration, sections for α-SMA staining were incubated in PBS/0.02% Triton

X-100 for 30 min at room temperature before primary antibody incubation. All procedures were protected from light. Sections were examined with a confocal laser scanning microscope.

Analysis of Angiogenic Factor Levels in Supernatants from B16-LacZ Cells and MSCs

To measure the levels of angiogenic factors secreted by B16-LacZ cells and MSCs, B16-LacZ cells alone (1.0×10^6 cells), MSCs alone (1.0×10^6 cells) or both B16-LacZ cells and MSCs (1.0×10^6 cells each) were cultured for 24 h in 10 mL DMEM/10% FBS media. The media were then collected and clarified by centrifugation (1,000*g*, 5 min), and the resulting supernatants were used for analysis. Concentrations of vascular endothelial growth factor (VEGF), macrophage inflammatory protein-2 (MIP-2; functional homolog of human interleukin [IL]-8), macrophage colony-stimulating factor (M-CSF), leukemia inhibitory factor (LIF), IL-15, IL-18, basic fibroblast growth factor (bFGF), monokine induced by interferon γ (MIG) and platelet-derived growth factor (PDGF) were determined with the Bio-Plex cytokine assay (Bio-Rad, Hercules, CA, USA) using a Luminex 200 (Luminex, Austin, TX, USA).

Statistical Analysis

Results are expressed as the mean ± standard deviation (SD). Comparisons between groups were performed using a two-tailed Student *t* test. Linear regression curves were produced using the Pearson correlation. *P* values <0.05 indicated statistical significance.

RESULTS

In Vitro-Cultured Mesenchymal Cells Express MSC Markers

Mouse bone marrow–derived MSC cultures were established from bone marrow cells isolated in C57BL/6 mice. Phenotypically, MSCs were characterized by being negative for expression of the CD34 and CD45 hematopoietic cell markers and positive for Sca-1, CD90 and CD44. Flow cytometric analysis revealed that cultured MSCs were positive for Sca-1, CD90 and low expression of CD44, but negative for CD34 and CD45 (Figure 1A), as expected. The MSCs exhibited a spindle-shaped morphology in culture (Figure 1B) and have been reported to differentiate into adipocytes and osteocytes (28). These results were consistent with previous reports and indicated that the established cell line indeed consisted of MSCs (29).

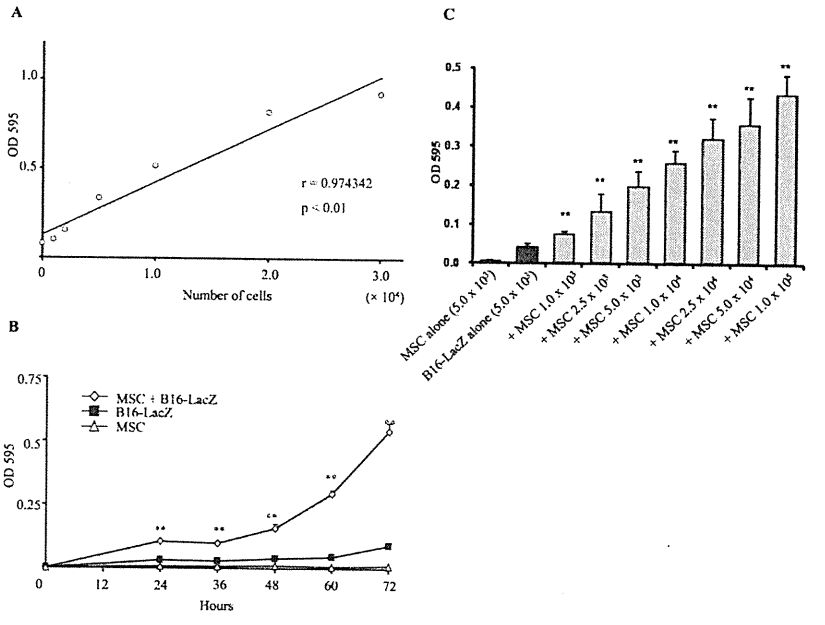

Figure 2. Proliferation of B16-LacZ cells cocultured with mesenchymal stromal cells (MSCs). (A) Standard curve correlating LacZ expression with cell numbers. B16-LacZ cells were seeded on 96-well plates at different cell numbers. After 24 h, β-galactosidase protein levels were analyzed in each well by measuring the absorbance at 595 nm using a microplate reader, as described in "Materials and Methods." (B) B16-LacZ cells were cultured with MSCs at a 1:1 ratio. β-Galactosidase protein expression was measured at the indicated time points (n = 5; $^{**}P < 0.01$). (C) B16-LacZ cells were incubated with MSCs at different ratios. β-Galactosidase protein expression was measured after 48 h (n = 8; $^{**}P < 0.01$). Q5

Coculture with MSCs Promotes Proliferation of B16-LacZ Cells *In Vitro*

We next analyzed whether MSCs could promote proliferation of the murine melanoma cell line B16-LacZ in an *in vitro* coculture model. Initially, a linear regression standard curve was generated to correlate the number of B16-LacZ cells with absorbance at 595 nm (OD_{595}). The assay was selective for B16-LacZ cells, because only this cell line expressed β-galactosidase (Figure 2A). Results from this analysis revealed that coculture of B16-LacZ cells with MSCs led to a marked increase in proliferation of B16-LacZ cells compared with B16-LacZ cells cultured alone (Figure 2B). After 48 h, the number of cells grown under coculture conditions was 3.6-fold greater than that of B16-LacZ cells cultured alone. On the basis of these results, we next analyzed the dose-response effect of MSCs on B16-LacZ proliferation (Figure 2C). These results showed that proliferation of B16-LacZ cells increased in accordance with the number of MSCs present in the coculture.

MSCs Promote B16-LacZ Cell Proliferation in the Absence of Direct Contact

To determine whether direct contact between B16-LacZ cells and MSCs is re-

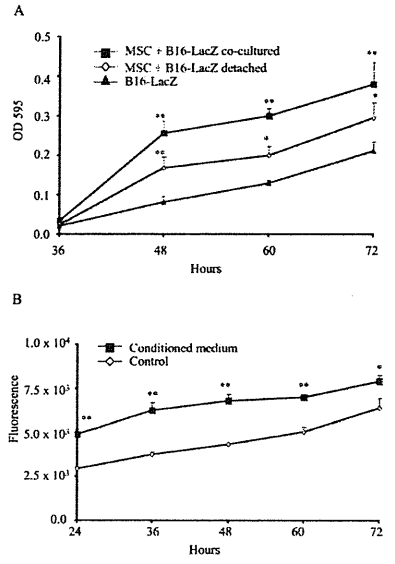

Figure 3. Effects of MSCs on B16-LacZ cell proliferation in the absence of direct contact. (A) B16-LacZ cells and MSCs were cultured together but were separated by a bulkhead consisting of a cell disk. Absorbance at 595 nm was determined at the indicated time points (n = 7; $*P < 0.05$; $**P < 0.01$). (B) B16-LacZ cells were cultured in conditioned medium from MSCs. Cell proliferation was measured using the Alamar Blue assay as described in the "Materials and Methods" (n = 7; $*P < 0.05$; $**P < 0.01$).

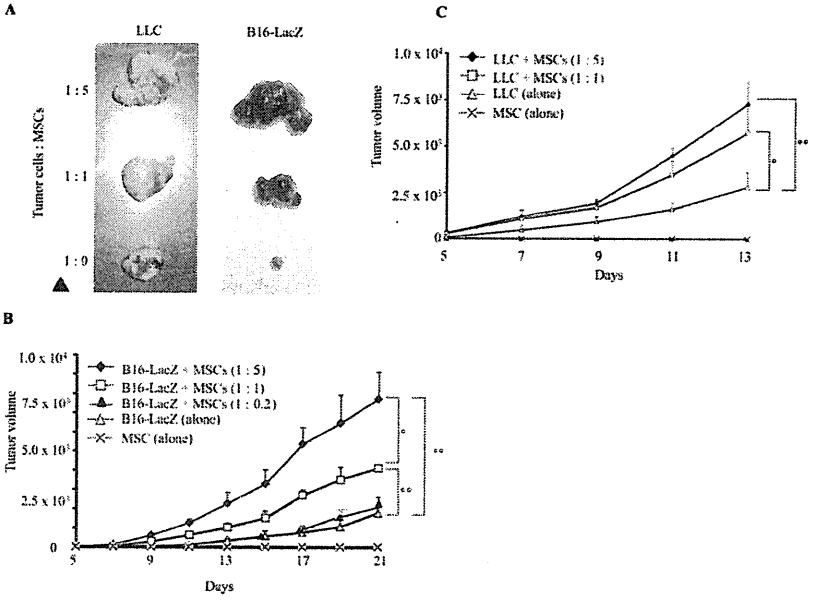

Figure 4. Analysis of tumors derived from xenografts of B16-LacZ cells or LLCs co-injected with MSCs. (A) Representative photographs of B16-LacZ tumors and LLC tumors. (B) B16-LacZ cells and MSCs were co-injected into the right side of the abdomen of C57BL/6 mice at a ratio of 1:0.2, 1:1 or 1:5. Tumor volume was calculated at 2-day intervals (n = 7; $*P < 0.05$; $**P < 0.01$). (C) LLCs and MSCs were co-injected as described for B16-LacZ cells, and tumor volume was calculated at 2-day intervals (n = 7; $*P < 0.05$, $**P < 0.01$).

quired for stimulation of B16-LacZ cell proliferation, cell growth in the absence of direct contact was investigated using cell disks and conditioned medium. Although the magnitude of stimulation of cell proliferation cannot be directly compared between cocultured cells and cells cultured in the absence of direct contact because of differences in growth conditions, a 2.3-fold increase in proliferation of B16-LacZ cells occurred in the presence of MSCs cultured on cell disks ($P < 0.01$; Figure 3A), and a 1.4-fold increase occurred in the presence of conditioned media ($P < 0.01$; Figure 3B) at 48 h. These values were slightly lower than the 6.4-fold increase in proliferation that occurred under conditions of 60-h direct contact in cocultures (see Figure 2B). To characterize the mechanisms underlying these changes in cell proliferation, we performed cell cycle analysis using flow cytometry. However, no obvious change in the cell cycle distributions of the cancer cells was apparent at the time points analyzed (data not shown).

MSCs Derived from Bone Marrow Promote Tumor Growth *In Vivo*

B16-LacZ cells and LLC cells, a lung carcinoma cell line, were used to assess the effects of MSCs on tumor promotion and growth in an *in vivo* model. Mixtures containing each of these cell types, along with MSCs, at ratios of 1:0.2, 1:1 and 1:5, were subcutaneously injected into syngeneic C57BL/6 mice, and tumor formation and growth were assayed. At day 21 after tumor inoculation, mice injected with B16-LacZ cells and MSCs at 1:1 and 1:5 ratios exhibited 2.3-fold ($P < 0.01$) and 4.3-fold ($P < 0.01$) greater tumor volumes, respectively, than mice injected with B16-LacZ cells alone (Figure 4A, B). However, tumor ratio of 1:0.2 did not increase tumor size compared with B16-LacZ cells alone (see Figure 4B). At day 13 after tumor inoculation, mice injected with LLCs and MSCs at 1:1 and 1:5 ratios exhibited 2.1-fold ($P < 0.05$) and 2.6-fold ($P < 0.01$) greater tumor volumes, respectively, compared with mice injected with LLCs alone (Figure 4A, C). Injection of MSCs alone did not result in tumor formation. Mixtures of B16-LacZ cells and another MSC cell line, TSt-4, derived from fetal thymus tissue, were also injected into C57BL/6 mice to assess the tumor growth effect of MSCs from a different origin. However, we observed no stimulatory or inhibitory effect on B16-LacZ tumor growth by TSt-4 MSCs at 1:1 and 1:5 ratios (data not shown). To exclude the possibility that increased tumor growth was due to immunosuppression caused by MSCs, B16-LacZ cells and/or MSCs were subcutaneously injected into BALB/c nude mice. Similar to the re-

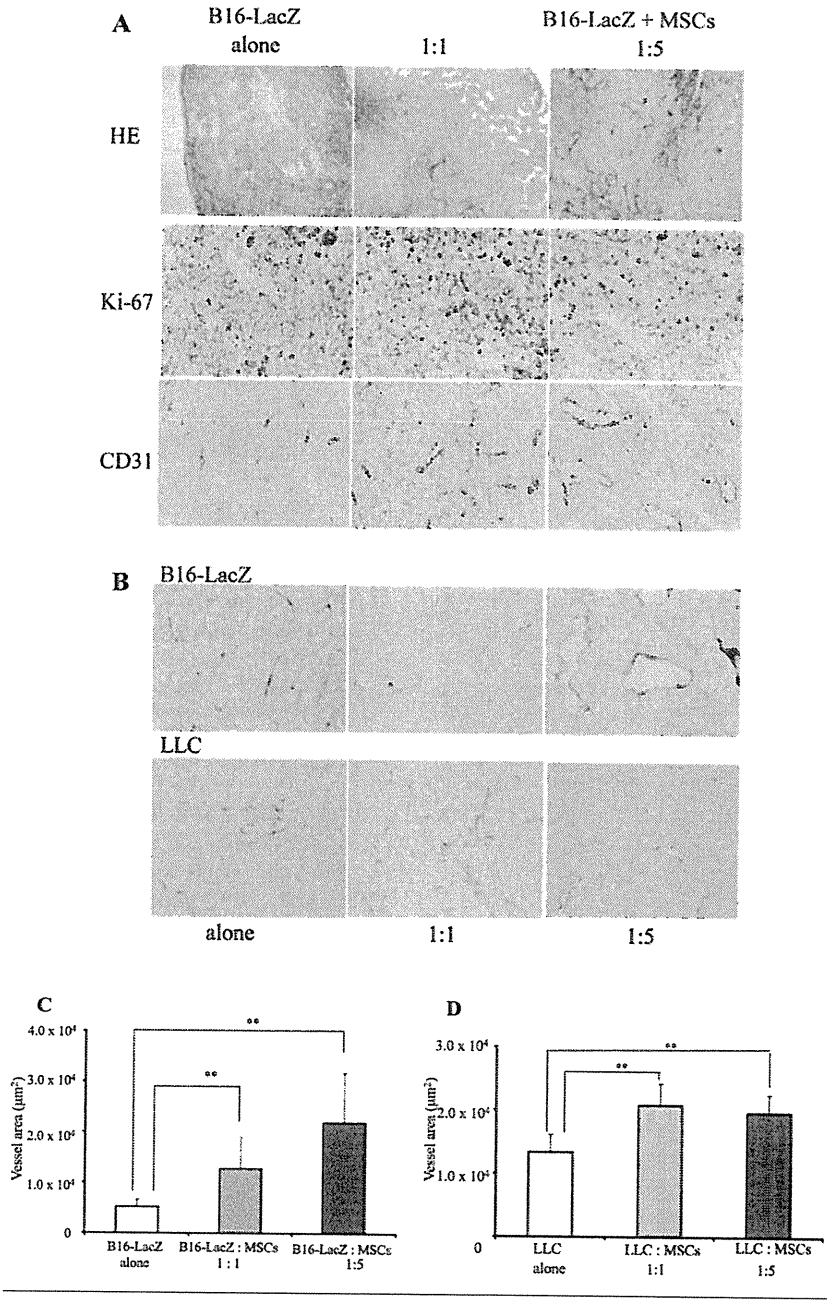

Figure 5. Analysis of B16-LacZ tumors in xenograft tumor models in the presence and absence of co-injected MSCs. (A) Photographs of tumors generated by injection of B16-LacZ alone or by co-injection of B16-LacZ cells with MSCs. On day 21, tumors were stained with hematoxylin and eosin, a Ki-67 antibody and a CD31 antibody. (B–D) Quantitative analyses of tumor angiogenesis. When tumors reached approximately 1 cm^3, they were removed, fixed and stained with a CD31 antibody (B). Microvessel density in tumor cryosections was analyzed by visualization of CD31 staining at 200× magnification. Microvessel density was quantified using the ImageJ software (n = 10; $^*P < 0.05$; $^{**}P < 0.01$). (C) B16-LacZ. (D) LLC. Q7

sults described above for syngeneic mice, co-injection of B16-LacZ cells and MSCs caused a significant increase in tumor volume compared with injection of B16-LacZ cells alone in nude mice ($P < 0.05$; data not shown).

MSCs Promote Tumor Growth *In Vivo* by Increasing Angiogenesis

To investigate mechanisms of tumor promotion by MSCs, we analyzed B16-LacZ + MSC tumors on day 21 (Figure 5). Hematoxylin and eosin staining revealed a massive necrotic area in B16-LacZ alone tumors, but not in B16-LacZ + MSC tumors (Figure 5A). *In vivo* analysis of cell proliferation using Ki-67 labeling was compared between B16-LacZ alone and B16-LacZ + MSC tumors (see Figure 5A). Percentages of Ki-67–positive cells in B16-LacZ alone tumors, B16-LacZ + MSC tumors at a 1:1 ratio and B16-LacZ + MSC tumors at a 1:5 ratio were 44.3 ± 5.1, 49.1 ± 3.4 and 42.4 ± 7.8, respectively, and were not significantly different. Thus, we hypothesized that MSCs may promote tumor growth by increasing angiogenesis. To assess whether MSCs promote angiogenesis, cryosections from tumors were stained with an antibody directed against CD31 to visualize blood vessels (see Figure 5A). Blood vessels were richer in B16-LacZ + MSC tumors (at ratios of 1:1 and 1:5) than in B16-LacZ alone tumors on day 21.

For optimal quantitative analysis of angiogenesis, we stained smaller tumors (around 1 cm^3) with CD31 antibody instead of large tumors on day 21. Blood vessel density was then analyzed by quantification of $CD31^+$ areas. Results from this analysis revealed that vessel area was increased in mice co-injected with B16-LacZ cells and MSCs (at ratios of 1:1 and 1:5) compared with mice injected with B16-LacZ cells alone ($P < 0.01$; Figure 5B, C). Similar results were observed when LLCs were used in place of B16-LacZ cells ($P < 0.01$). However, no significant difference was observed in mice co-injected with different ratios of cancer cells to MSCs (1:1 and 1:5, respectively; Figure 5B, D).

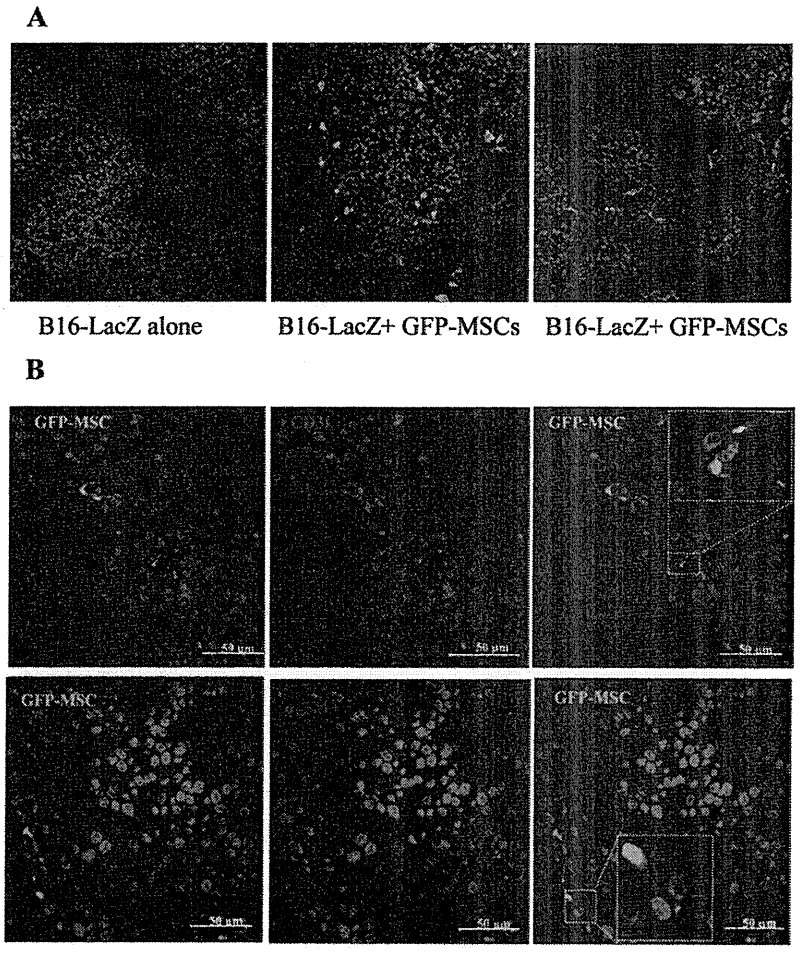

Figure 6. Presence and differentiation of MSCs in the tumors. (A) GFP-MSCs present and randomly distributed in the tumors on day 21 generated by co-injection of B16-LacZ cells and GFP-expressing MSCs. (B) GFP-MSCs closely localized to tumor vessels coexpressed the endothelial marker CD31, but did not coexpress the pericyte marker α-SMA.

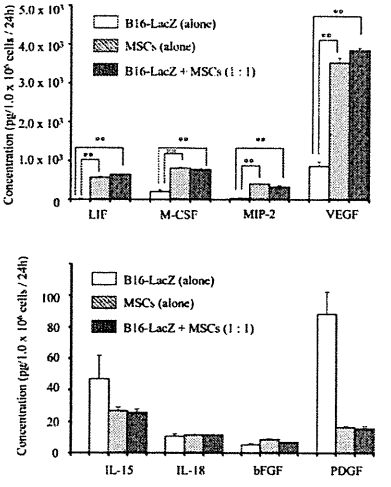

Figure 7. Expression of proangiogenic factors by MSCs. Secreted levels of LIF, M-CSF, MIP-2, VEGF (*upper panel*), IL-15, IL-18, bFGF and PDGF (*lower panel*) were analyzed in media from B16-LacZ cells (1.0×10^5 cells/mL), MSCs (1.0×10^5 cells/mL) or cocultures of B16-LacZ cells and MSCs (1.0×10^5 cells/mL each). Concentrations were analyzed using a Luminex 200 (n = 3; $^{**}P < 0.01$).

Differentiation of MSCs in the Tumors

To assess the role of MSCs in tumor promotion, MSCs from GFP mice (GFP-MSCs) were co-injected with B16-LacZ cells at a ratio of 1:1 into mice. Although GFP-MSCs presented in tumor tissues on day 21 (Figure 6A), the number of MSCs was quite low and MSCs were randomly distributed in tumor tissues. Some MSCs were closely presented at vessel structures. To assess differentiation and its association with tumor vessels, tumor tissues were stained with a CD31 antibody, as an endothelial marker (Figure 6B), or an_Q9α-SMA antibody, as a pericyte marker. Confocal microscopy revealed that some MSCs that were closely presented in the tumor vasculature expressed CD31 but not α-SMA.

MSCs Secrete Several Angiogenic Cytokines

On the basis of the observation that MSCs promoted angiogenesis *in vivo*, we next assessed the levels of several secreted proangiogenic factors in media from MSCs and B16-LacZ cells. Levels of VEGF, MIP-2, M-CSF, LIF, IL-15, IL-18, bFGF, MIG and PDGF secreted by B16-LacZ cells (1.0×10^6 cells) alone, MSCs (1.0×10^6)Q3 alone and cocultures of B16-LacZ cells and MSCs (1.0×10^6 cells each) were analyzed. Results from this analysis showed that MSCs secreted higher levels of LIF, M-CSF, MIP-2 and VEGF than tumor cells (Figure 7, *upper panel*). Both B16-LacZ cells and MSCs secreted little IL-15, IL-18, bFGF, MIG or PDGF (Figure 7, *lower panel*).

DISCUSSION

In this study, we demonstrated that MSCs promote tumor cell proliferation *in vitro* and tumor growth *in vivo*. In both the presence and absence of direct contact, MSCs stimulated proliferation of B16-LacZ cells *in vitro*. Furthermore, combined administration of MSCs and tumor cells (B16-LacZ cells or LLCs) promoted tumor growth by enhancing angiogenesis in syngeneic tumor models.

This enhanced neovascularization can likely be attributed to direct support of neovascularization by MSCs and to secretion of angiogenic factors, including VEGF and others, by MSCs.

Our results suggest that both direct cell–cell contact and soluble factors likely play important roles in MSC-mediated stimulation of tumor cell proliferation *in vitro*, although we were not able to determine the molecules responsible for this phenotype. To date, few *in vitro* studies have assessed the effects of MSCs on tumor cell proliferation, because of the difficulty in distinguishing tumor cell proliferation from that of MSCs under coculture conditions. Sasser *et al.* (30) demonstrated that MSCs enhance proliferation of human breast cancer cells through the use of tumor cells that expressed stable red fluorescence. Similar to our β-galactosidase–based system, measurement of fluorescence intensity could distinguish between proliferation of fluorescent tumor cells and human MSCs in cocultures (30). Results from this study indicated that stimulation of tumor cell proliferation by human MSCs was solely due to secreted soluble factors, in contrast to our results suggesting that both direct contact and soluble factors play a role in stimulating proliferation. Another study demonstrated that treatment of pancreatic tumor cells with conditioned media from cancer-associated stromal fibroblasts enhanced cell proliferation *in vitro*; however, effects in cocultures containing both fibroblasts and tumor cells were not examined (4). Secreted IL-6 from fibroblasts was reported to enhance the rate of cancer cell proliferation in a previous study (5). Thus, IL-6 may represent one of the soluble factors partially responsible for stimulation of cell proliferation in B16-LacZ cells. Although these studies demonstrated MSC-mediated stimulation of tumor cell proliferation *in vitro*, none of them analyzed changes in the cell cycle. We did not observe any change of cell cycle distribution. This negative observation may have been because of using non-synchronized cells. Nevertheless, further investigation is needed to identify the precise molecules that mediate this effect.

Subcutaneous co-injection of tumor cells and MSCs resulted in more rapid tumor growth in mice compared with injection with tumor cells alone in assays using either B16-LacZ or LLC cells. Increased tumor growth was independent of the mouse strain background; indeed, similar effects were observed in both syngeneic mice and nude mice. The MSC cell line TSt-4 derived from fetal thymus tissue did not affect B16-LacZ tumors *in vivo*. The reported effects of MSCs on progression of primary tumors have been both pro- and antitumorigenic, but variability in these results, including ours, could be attributable to differences in the sources of the MSCs and the type of tumor model used for analysis. For example, intravenous injection of human MSCs into Kaposi's sarcoma-bearing nude mice inhibited tumor growth (26). MSCs also decreased proliferation of Kaposi's sarcoma cells *in vitro* under conditions of direct contact through inhibition of Akt signaling. Human MSCs were found to inhibit proliferation of a leukemia cell line and a small cell–lung cancer cell line *in vitro*, whereas tumor cells grew significantly faster when co-injected with MSCs into nonobese diabetic severe combined immunodeficient mice compared with injection of tumor cells alone (31). However, MSC-mediated inhibitory effects have only been observed in a few models, and most studies reported protumorigenic effects, consistent with our findings. Note also that immunosuppressive effects caused by MSCs were shown to promote B16 tumor growth in an allogeneic mouse model (32). However, this was not the case in our study, because we observed no difference in the effect of MSCs on tumor growth between nude and syngeneic mice.

We observed neither a change in the Ki-67 labeling index in the B16-LacZ + MSC tumors nor a high number of MSCs in the tumor tissues. These observations suggest that tumor promotion by MSCs was not due to stimulated tumor cell growth or an increased number of MSCs. We demonstrated that MSCs strongly stimulate tumor angiogenesis, likely through secretion of several angiogenic factors. The effects of MSCs on the tumor vasculature remain unclear and are likely to be complex (33,34). We hypothesize that MSCs exert paracrine effects on endothelial cells via secreted growth factors and cytokines, directly contributing to blood vessel formation in the tumor microenvironment. MSCs secrete many proangiogenic factors, including VEGF, IL-6, transforming growth factor-β and IL-8 (24,34–36), and secretion of these proangiogenic factors was shown to be significantly enhanced by treatment with conditioned media from tumor cells (24). However, we did not observe enhanced secretion of these factors from MSCs as a result of coculture with tumor cells, although MSCs did secrete higher amounts of proangiogenic factors than tumor cells. VEGF expression in MSCs can be enhanced by hypoxia, a common phenomenon in tumor tissues (37). Together, these data and our findings suggest that MSCs play a key role in tumor neovascularization.

Another contribution of MSCs to the tumor vasculature occurs through the support of vascular formation in tumor tissues. In the present study, we attempted to investigate the differentiation state of MSCs after co-injection with tumor cells using GFP-MSCs. Some MSCs closely presented to the tumor vasculature and expressed the endothelial cell marker CD31, but not the pericyte marker α-SMA. Grafted MSCs were shown to integrate into tumor vessel walls and express pericyte markers, but not endothelial markers, suggesting that MSCs in tumor tissues differentiate into pericytes and contribute to the tumor vasculature (25). Although this report was different from ours, these studies suggest that MSCs directly support the tumor vasculature by differentiating into endothelial cells, pericytes or other types of cells. Additionally, grafted MSCs were reported to differentiate into tumor-

associated fibroblasts and to contribute to tumor progression (38).

In conclusion, results from this study demonstrate that MSCs stimulate tumor cell proliferation *in vitro* and tumor growth *in vivo*. Enhanced tumor growth in syngeneic mouse models by MSCs may be, in part, due to promotion of tumor neovascularization by directly supporting the tumor vasculature and secreting proangiogenic factors. These results suggest that MSCs play an important role in tumor progression.

ACKNOWLEDGMENTS

This work was supported in part by grants-in-aid for scientific research from the Ministry of Education, Science, Sports, Culture and Technology, Japan (numbers 16022206 and 20390229).

DISCLOSURE

The authors declare that they have no competing interests as defined by *Molecular Medicine*, or other interests that might be perceived to influence the results and discussion reported in this paper.Q4

REFERENCES

1. Dvorak HF. (1986). Tumors: wounds that do not heal. Similarities between tumor stroma generation and wound healing. *N. Engl. J. Med.* 315:1650–9.
2. Bissell MJ, Radisky D. (2001). Putting tumours in context. *Nat. Rev. Cancer.* 1:46–54.
3. Karnoub AE, *et al.* (2007). Mesenchymal stem cells within tumour stroma promote breast cancer metastasis. *Nature.* 449:557–63.
4. Hwang RF, *et al.* (2008). Cancer-associated stromal fibroblasts promote pancreatic tumor progression. *Cancer Res.* 68:918–26.
5. Studebaker AW, *et al.* (2008). Fibroblasts isolated from common sites of breast cancer metastasis enhance cancer cell growth rates and invasiveness in an interleukin-6-dependent manner. *Cancer Res.* 68:9087–95.
6. Kim S, *et al.* (2009). Carcinoma-produced factors activate myeloid cells through TLR2 to stimulate metastasis. *Nature.* 457:102–6.
7. Grugan KD, *et al.* (2010). Fibroblast-secreted hepatocyte growth factor plays a functional role in esophageal squamous cell carcinoma invasion. *Proc. Natl. Acad. Sci. U. S. A.* 107:11026–31.
8. Paulsson J, *et al.* (2009). Prognostic significance of stromal platelet-derived growth factor beta-receptor expression in human breast cancer. *Am. J. Pathol.* 175:334–41.
9. Utispan K, *et al.* (2010). Gene expression profiling of cholangiocarcinoma-derived fibroblast reveals alterations related to tumor progression and indicates periostin as a poor prognostic marker. *Mol. Cancer.* 9:13.
10. Wels J, Kaplan RN, Rafii S, Lyden D. (2008). Migratory neighbors and distant invaders: tumor-associated niche cells. *Genes. Dev.* 22:559–74.
11. Direkze NC, *et al.* (2004). Bone marrow contribution to tumor-associated myofibroblasts and fibroblasts. *Cancer Res.* 64:8492–5.
12. Udagawa T, Puder M, Wood M, Schaefer BC, D'Amato RJ. (2006). Analysis of tumor-associated stromal cells using SCID GFP transgenic mice: contribution of local and bone marrow-derived host cells. *FASEB J.* 20:95–102.
13. Worthley DL, *et al.* (2009). Human gastrointestinal neoplasia-associated myofibroblasts can develop from bone marrow-derived cells following allogeneic stem cell transplantation. *Stem Cells.* 27:1463–8.
14. Pittenger MF, et al. (1999). Multilineage potential of adult human mesenchymal stem cells. *Science.* 284:143–7.
15. Prockop DJ. (1997). Marrow stromal cells as stem cells for nonhematopoietic tissues. *Science.* 276:71–4.
16. Campagnoli C, *et al.* (2001). Identification of mesenchymal stem/progenitor cells in human first-trimester fetal blood, liver, and bone marrow. *Blood.* 98:2396–402.
17. Karp JM, Leng Teo GS. (2009). Mesenchymal stem cell homing: the devil is in the details. *Cell Stem Cell.* 4:206–16.
18. Ortiz LA, *et al.* (2003). Mesenchymal stem cell engraftment in lung is enhanced in response to bleomycin exposure and ameliorates its fibrotic effects. *Proc. Natl. Acad. Sci. U. S. A.* 100:8407–11.
19. Lian Q, *et al.* (2010). Functional mesenchymal stem cells derived from human induced pluripotent stem cells attenuate limb ischemia in mice. *Circulation.* 121:1113–23.
20. Studeny M, *et al.* (2004). Mesenchymal stem cells: potential precursors for tumor stroma and targeted-delivery vehicles for anticancer agent. *J. Natl. Cancer Inst.* 96:1593–603.
21. Kidd S, *et al.* (2009). Direct evidence of mesenchymal stem cell tropism for tumor and wounding microenvironments using in vivo bioluminescent imaging. *Stem Cells.* 27:2614–23.
22. Klopp AH, *et al.* (2007). Tumor irradiation increases the recruitment of circulating mesenchymal stem cells into the tumor microenvironment. *Cancer Res.* 67:11687–95.
23. Coffelt SB, *et al.* (2009). The pro-inflammatory peptide LL-37 promotes ovarian tumor progression through recruitment of multipotent mesenchymal stromal cells. *Proc. Natl. Acad. Sci. U. S. A.* 106:3806–11.
24. Spaeth EL, *et al.* (2009). Mesenchymal stem cell transition to tumor-associated fibroblasts contributes to fibrovascular network expansion and tumor progression. *PLoS One.* 4:e4992.
25. Bexell D, *et al.* (2009). Bone marrow multipotent mesenchymal stoma cells act as pericyte-like migratory vehicles in experimental gliomas. *Mol. Ther.* 17:183–90.
26. Khakoo AY, *et al.* (2006). Human mesenchymal stem cells exert potent antitumorigenic effects in a model of Kaposi's sarcoma. *J. Exp. Med.* 203:1235–47.
27. Watanabe Y, *et al.* (1992) A murine thymic stromal cell line which may support the differentiation of CD4–8- thymocytes into CD4+8- alpha beta T cell receptor positive T cells. *Cell. Immunol.* 142:385–97.
28. Umezawa A, *et al.* (1992). Multipotent marrow stromal cell line is able to induce hematopoiesis in vivo. *J. Cell Physiol.* 151:197–205.
29. Annabi B, *et al.* (2003). Hypoxia promotes murine bone-marrow-derived stromal cell migration and tube formation. *Stem Cells.* 21:337–47.
30. Sasser AK, *et al.* (2007). Human bone marrow stromal cells enhance breast cancer cell growth rates in a cell line-dependent manner when evaluated in 3D tumor environments. *Cancer Lett.* 254:255–64.
31. Ramasamy R, *et al.* (2007). Mesenchymal stem cells inhibit proliferation and apoptosis of tumor cells: impact on in vivo tumor growth. *Leukemia.* 21:304–10.
32. Djouad F, *et al.* (2003). Immunosuppressive effect of mesenchymal stem cells favors tumor growth in allogeneic animals. *Blood.* 102:3837–44.
33. Beckermann BM, *et al.* (2008). VEGF expression by mesenchymal stem cells contributes to angiogenesis in pancreatic carcinoma. *Br. J. Cancer.* 99:622–31.
34. Otsu K, *et al.* (2009). Concentration-dependent inhibition of angiogenesis by mesenchymal stem cells. *Blood.* 113:4197–205.
35. Gunn WG, *et al.* (2006). A crosstalk between myeloma cells and marrow stromal cells stimulates production of DKK1 and interleukin-6: a potential role in the development of lytic bone disease and tumor progression in multiple myeloma. *Stem Cells.* 24:986–91.
36. Romieu-Mourez R, *et al.* (2009). Cytokine modulation of TLR expression and activation in mesenchymal stromal cells leads to a proinflammatory phenotype. *J. Immunol.* 182:7963–73.
37. Potier E, *et al.* (2007). Hypoxia affects mesenchymal stromal cell osteogenic differentiation and angiogenic factor expression. *Bone.* 40:1078–87.
38. Mishra PJ, *et al.* (2008). Carcinoma-associated fibroblast-like differentiation of human mesenchymal stem cells. *Cancer Res.* 68:4331–9.

Queries

Q1: Can CAG-EGFP be expanded?

Q2: Please expand GFP.

Q3: Should "1.0 × 10^6" read "1.0 × 10^6 cells"?

Q4: Please confirm that this disclosure statement is correct. If you do have something to declare, please provide that information.

Q5: Fig. 2: Please define OD595. Optical density absorbance at 595 nm?

Q6: Is a symbol such as the plus sign missing here?

Q7: Is this line correct as edited?

Q8: Please provide a new figure 1 with legible axes at a resolution of at least 300 dpi.

Q9: Is something missing here?

血液内科，63(5)：614-620，2011

Lecture

解　説

WHO分類2008に基づく急性混合性白血病の臨床像の解析*

伊　藤　薫　樹**

Key Words : mixed-phenotype acute leukemia, WHO 2008 classification, biphenotypic acute leukemia, clinical features and outcome

はじめに

急性混合性白血病(mixed-phenotype acute leukemia；MPAL)は，WHO分類2008の分化系統不明瞭な急性白血病に属する稀な疾患である[1]．MPALは，これまでEuropean Group for the Immunological Characterization of Leukemias (EGIL)のスコアリングシステム[2]に基づいてbiphenotypic acute leukemia(BAL)として診断されたが，WHO分類2008では，分化系統を判定するための新たな基準を用いて，細胞遺伝学的異常により分類される．しかしながら，本分類には，MPALの臨床学的意義や治療戦略についての具体的な記載はない．ここでは混乱を避けるために，WHO分類2008により定義された急性混合性白血病をMPAL，それ以前のものをBALとして記載する．本稿では，最近の知見を交えてWHO分類2008に基づくMPALの疾患概念と臨床学的特徴を中心に解説する．

歴史的背景

急性混合性白血病の記載は，モノクローナル抗体が白血病細胞の系統や分化度を調べるために用いられるようになった1980年代に始まった．しかしながら，WHO分類2008にMPALとして記載されるまでには，分化系統の決定に重要な抗原特異性の問題のために改訂が繰り返された経緯がある．Mirroらは，123例の小児白血病を対象に骨髄系とリンパ系の両者の特徴を有する急性白血病の頻度と意義を報告した[3]．当時はリンパ系マーカーとしてCD2, CD5, CD10が，骨髄系マーカーとしてCD11b, CD13, CD15が用いられていた．これらは現在，系特異的といえるマーカーではない．この定義を用いた結果，全体の20%が急性混合性白血病と診断された．その後，より多くのモノクローナル抗体が用いられるようになり，急性混合性白血病の診断基準が提唱されるに至った．1991年，CatovskyらはBALの診断のためのスコアリングシステムを提唱した[4]．これにより診断されたBALの臨床的特徴が解析され，BALは通常の急性白血病とは異なることが示唆された．1995年，EGILはCatovskyの診断基準に基づいてBALを含めた急性白血病の免疫学的分類のためのスコアリングシステムを提唱した[2]．表1にそのスコアリングシステムを示す．各分化系統を特定する抗原が点数化されているのが特徴である．このスコアリングシステムの改訂版がWHO分類2001に引き継がれた[5]．しかしながら，この改訂システムを導入した際に分化系統を特定するための点数に誤りがあったため，混乱と過剰な診断をもたらした[6]．その後，BAL症例の集積により臨床学的特徴や細胞遺伝学的特徴が明らかになるにつれてEGILの診断分類の限界が認識され，WHO分類2008では，分化系統

* Clinical and laboratory features and outcome of mixed-phenotype acute leukemia according to WHO 2008 classification.

** Shigeki ITO, M.D., Ph.D.: 岩手医科大学内科学講座血液・腫瘍内科分野〔〒020-8505 盛岡市内丸19-1〕; Hematology & Oncology, Department of Internal Medicine, Iwate Medical University School of Medicine, Morioka 020-8505, JAPAN

の判定のための新基準に基づいた新たな分類が提唱された[1]．

MPALの診断

WHO分類2008では，MPALは表2に示すように，分化系統不明瞭な急性白血病の中に含まれる．MPALは，2系統以上の形質を有する急性白血病であるが，この中には芽球が2系統以上存在するbilineal(3系統であればtrilineal)の白血病と，1つの芽球上に2系統以上の抗原が発現するbiphenotypic(3系統であればtriphenotypic)の白血病があり，その両者を含む．表3に各分化系統を特定する基準を示す[1]．本基準では，EGILやWHO分類2001の基準とは異なり系統の判定のための点数化が除かれている．T細胞系のマーカーはCD3のみである．細胞質内CD3(cytCD3)あるい

表1　EGILの急性混合性白血病の改訂スコアリングシステム

ポイント	B細胞系	T細胞系	骨髄系
2	CD79a cytIgM cytCD22	(cyt)CD3 TCR(α/β) TCR(γ/δ)	MPO
1	CD19 CD10 CD20	CD2 CD5 CD8 CD10	CD117 CD13 CD33 CDw65
0.5	TdT CD24	TdT CD7 CD1a	CD14 CD15 CD64

B細胞系あるいはT細胞系のいずれかと骨髄系において，ポイントの合計が2を超えた場合に急性混合性白血病と診断する．
Cyt：cytoplasmic, MPO：myeloperoxidase, TCR：T-cell receptor, TdT：terminal deoxynucleotidyl transferase
（文献[2]より引用改変）

表2　WHO分類2008：分化系統不明瞭な急性白血病の分類

1. 未分化急性白血病
   Acute undifferentiated leukaemia
2. Ph染色体(*BCR-ABL1*再構成)を伴う急性混合性白血病
   Mixed phenotype acute leukaemia with t(9;22)(q34;q11.2)；*BCR-ABL1*
3. *MLL*遺伝子再構成を伴う急性混合性白血病
   Mixed phenotype acute leukaemia with t(v;11q23)；*MLL* rearranged
4. 急性混合性白血病，B/骨髄性，非特定型
   Mixed phenotype acute leukaemia, B/myeloid, NOS
5. 急性混合性白血病，T/骨髄性，非特定型
   Mixed phenotype acute leukaemia, T/myeloid, NOS
6. 急性混合性白血病，その他稀少型
   Mixed phenotype acute leukaemia, NOS-rare types
7. その他の系統を特定できない白血病
   Other ambiguous lineage leukaemias

表3　分化系統不明瞭な急性白血病の系統特定のための判定基準

細胞系統	マーカー
骨髄系	ミエロペルオキシダーゼ （フローサイトメトリー，免疫染色，もしくは細胞化学） あるいは 単球系への分化 （非特異的エステラーゼ染色のびまん性陽性，もしくはCD11c, CD14, CD64, リゾチームの2つ以上のマーカーが陽性）
T細胞系	細胞質内CD3 （フローサイトメトリーのみ．免疫染色は不可） あるいは 表面CD3
B細胞系	CD19強陽性かつCD79a, 細胞質内CD22, CD10の1つ以上が強陽性 あるいは CD19弱陽性かつCD79a, 細胞質内CD22, CD10の2つ以上が強陽性

（文献[1]より引用改変）

は細胞表面CD3が陽性であればよい．骨髄系はミエロペルオキシダーゼ(myeloperoxidase；MPO)または単球系への分化所見(非特異的エステラーゼ染色のびまん性陽性パターン，もしくはCD11c, CD14, CD64, リゾチームのうち少なくとも2つ以上陽性)が認められる必要がある．一方，B細胞系は単独で特異的なマーカーがないため，CD19発現が強陽性の場合はCD10, CD79a, cytCD22のB細胞系マーカーのうちいずれか1つ以上の強発現を，CD19発現が弱陽性であった場合は少なくともほかに2つ以上のB細胞系マーカーの強発現を必要としているのが特徴である．また，以上からMPALの発現抗原基準を満たしたとしても，他の急性白血病の診断分類に当てはまる場合はMPALから除外される点に注意が必要である．たとえば，t(8;21)(q22;q22)を有する急性骨髄性白血病(acute myeloid leukemia；AML)ではCD19を発現することが稀ではないため[7]，MPALと診断される可能性がある．この場合は，t(8;21)を伴うAMLに分類すべきである．同様に，t(15;17)，inv(16)を伴うAML，*FGFR1*遺伝子異常を持つ白血病，慢性骨髄性白血病の急性転化，骨髄異形成症候群(myelodysplastic syndromes；MDS)または白血病化MDS, 化学療法などによる二次性白血病などは除外される．WHO分類2008では，これまでのBALの核型異常に関する報告の多くがt(9;22)あるいは*MLL*遺伝子再構成であったため，表2に示すように，独立したカテゴリーとして扱われている．また，これらの染色体(遺伝子)異常を伴わないMPALを非特定型(not otherwise specified；NOS)として別のカテゴリーとしている[1]．

臨床学的特徴

症状は，通常の急性白血病で認められるものと同様で，正常の造血抑制を反映して貧血症状，感染症状，出血傾向を認める[8]．多くは末梢血に芽球が出現し，白血球数は増加する[8]．EGILの診断基準によるBALの頻度は急性白血病の2～5％とされるが，最近の成人の白血病を対象にした検討では1.8％と報告されている[9][10]．小児と成人の間での頻度の違いはない[9][11]．WHO分類2008に基づいたMPALの頻度はEGILで診断されたBALの頻度よりも少ないとされる．実際，Al-Seraihyらの633例の小児白血病を対象にした後方視的な診断によると，EGILによるBALが3.8％であったのに対して，WHO分類2008によるMPALが1.7％であった[12]．さらに他の多くの解析でもMPALの頻度はEGILによるBALの頻度よりも少なかった[13]．これは，前述したように転座型白血病，化学療法に伴う二次性白血病などがWHO分類2008ではそれぞれ別のカテゴリーに分類されていることや，MPAL診断のための抗原基準が厳密になったことに起因すると考えられる．最近，Matutesらは，WHO分類2008により診断された100例のMPALの臨床学的な調査結果を報告した[14]．MPALの頻度は急性白血病の0.5～1％であった．表4にその臨床学的特徴を示す．男女比は1.6と男性に多く，68％が成人(＞15歳)であった．形態学的には，評価された90例中39例が急性リンパ性白血病(acute lymphoblastic leukemia；ALL)，38例がAMLに分類され，AMLでは多くがM1あるいはM5であった．残りの13例は小型と大型の2種類の芽球が存在し，形態分類は困難であったと報告している．著者らは，2種類の芽球が認められる症例以外では形態学的にMPALを診断することは困難であると述べている．

MPALの発現抗原の特徴

ほとんどのMPALはCD45抗原を発現し，造血幹細胞マーカーであるCD34, CD38, TdT, HLA-DRを発現する[8]．これらに加えて，骨髄系(My)，B細胞系(B)，T細胞系(T)の分化マーカーのうち，いずれか2系統の組み合わせ(B＋My, T＋My, B＋T)あるいは3系統すべて(B＋T＋My)が発現する．MatutesらによるMPAL 100例の発現抗原の解析では，B＋Myが59％と最も多く，次いで，T＋Myが35％であった．B＋Tは4％，B＋T＋Myは2％に認められた(表4)．また，TdTは89％に，HLA-DRは92％に，CD34は74％の症例に認められた．B＋MyとT＋Myの間で臨床的特徴の差異が検討されたが，年齢，性別，形態に明らかな違いは認められなかった．一方，B＋Tでは小児に多く(4例中3例)，B＋T＋Myの2例はいずれも成人例であった(表4)[14]．以上から，MPALの発現抗原は，B＋Myが半数以上と最も多く，T＋Myが1/3を占め，その他のパ

表4　MPAL 100例の発現抗原パターンと臨床学的特徴

	B+My	T+My	B+T	B+T+My	全体数
数(%)	59(59%)	35(35%)	4(4%)	2(2%)	100
年齢(小児/成人)	18/38	6/27	3/1	0/2	27/68
性(男/女)	35/24	22/12	3/1	1/1	62/38
ALL	25	8	4	2	39
AML	22	15	0	0	38
AUL	7	6	0	0	13
MPO	55*	35	0	2	
CytCD3	0	35	4	2	
CD19	54§	0	4	2	
CD10	33/53	4/25	3	1	
CytCD22	45/54	0	2	2	
CD79a	34/38	4/15	2/2	1	

*4例はフローサイトメトリー法で検討されていない(細胞化学染色法で陽性)，§5例はCD19陰性であったが2つか3つ以上のBリンパ系マーカーが強陽性に発現.
ALL：acute lymphoblastic leukemia, AML：acute myeloid leukemia, AUL：acute undifferentiated leukemia, MPO：myeloperoxidase
(文献[14]より引用改変)

ターンはきわめて稀であると考えられるが，その発現抗原パターンの臨床的意義ははっきりしない.

細胞遺伝学的特徴

これまでMPAL特有の染色体異常の報告はない. OwaidahらによるEGILにより診断された23例のBALの検討では，68%になんらかのクローナルな異常を認め，32%は正常核型であった[9]. *MLL*遺伝子座を有する11q23の再構成が最も多く，次いでt(9;22)が認められた. そのほかには，6q, 5q, 12pの欠失が認められた[9]. Leeらは43例のBALを解析し，t(9;22)が最も多く32%に認められたと報告している[15]. これに対して，小児ではPh染色体陽性例は少なく，3%程度との報告がある[12]. Rubnitzらは，小児では5番，7番染色体異常が最も多く，12pの異常がそれに次いで多く認められたと報告した[16]. MatutesらによるMPALの検討では，100例中76例が解析対象となり，t(9;22)が15例(20%)に，*MLL*遺伝子再構成が6例(8%)に認められた[14]. また，複雑型染色体異常が24例(32%)に，他の異常が21例(27%)に認められた. 正常核型は10例(13%)と少なかった. 複雑型染色体異常に多く含まれていた異常は，del(6)，7番染色体異常〔7q−, −7, t(2;7)〕, −5/5q−であった. Gerrらは，EGIL基準によるBAL小児例に*EVT6/RUNX1*再構成が比較的多く認められたと報告したが[17]，MPALでは2例のみであった. これは，Gerrらの診断したBAL症例に，骨髄系抗原を発現したALLが含まれていたことによるのかもしれない. Matutesらは，染色体異常と年齢，細胞形態，発現抗原との関係を検討したが，有意な相関は認められなかった. しかしながら，Ph染色体はB+My型の成人MPALに，*MLL*遺伝子再構成は小児のMPALに多い傾向にあった[14]. 以上から，MPALは複雑型染色体異常，Ph染色体，*MLL*遺伝子再構成などの細胞遺伝学的な異常を伴うことが多いが，特異的な染色体異常はないものと思われる.

治療と予後

MPALに対する標準治療は確立されていない. 寛解導入療法についてもAMLに準じた方が良いのか，ALLとしてレジメンを選択すべきかのコンセンサスはなく，また，移植によって予後が改善するかも不明である[11]. Al-Seraihyらは，小児のBALに対してハイリスクALLに準じたレジメンを用いているが，骨髄性白血病にも有効な薬剤を組み込んでいる[12][18]. Killickらは，AMLとALLに用いる薬剤を組み合わせた治療を行ったが，早期死亡が多かったことを報告した[11]. Rubnitzらは，小児のBALに対して施行したALLに準じた治療が，AMLの治療に比べて寛解率が高かったと報告した(83% vs. 52%)[16]. さらにAMLに準

表5　MPAL 70例における臨床学的特徴と治療成績

	死亡数(N=40)	中央生存期間, 月 (95%CI)	有意差
小児(N=27)	8	139	$P<0.001$
成人(N=42)	31	11.8(5～13.5)	
細胞遺伝学的特徴			
Ph^+(N=12)	11	8(2～14)	Ph^+ vs. その他すべて, $P=0.002$
MLL(N=6)	2	undefined	
複雑型(N=21)	9	47	
その他(N=19)	10	30	
正常(N=7)	3	139	
不明(N=12)	5	3	
免疫学的特徴			
B+My(N=39)	23	13(0～35)	$P=0.7$
T+My(N=27)	15	18(0～55)	
B+T/B+T+My(N=4)	2	undefined	
治療			
ALL(N=27)	10	139(8～270)	ALL vs. その他すべて, $P=0.003$
AML(N=34)	22	11(8～14)	
その他(N=6)	5	3(0～6)	
治療なし/不明(N=3)	3		

(文献[14]より引用改変)

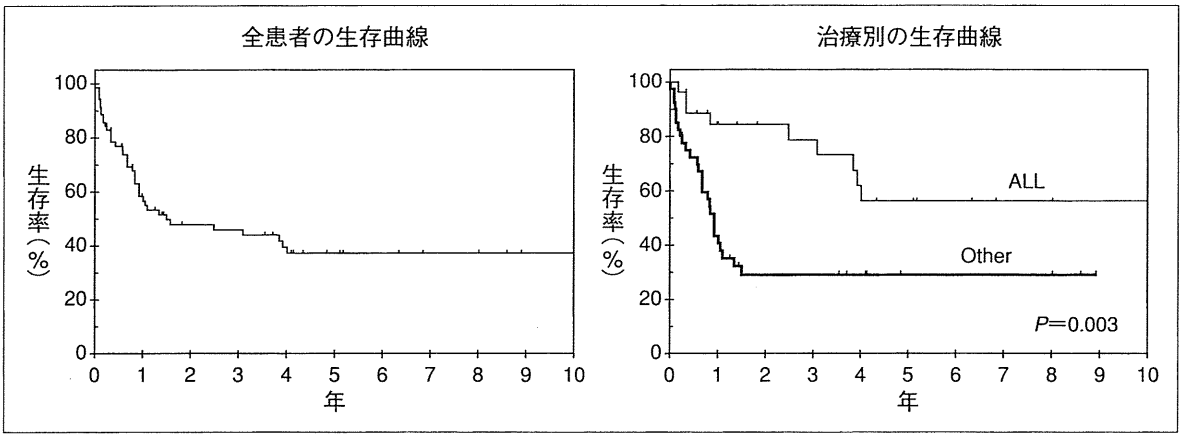

図1　MPALの生存曲線(全体と治療別)(文献[14]より引用改変)

じた治療で寛解に到達しなかった10例に対してALLに準じた治療を行い，8例が寛解に到達した[16]．Matutesらは，初回治療の情報が得られた67例のMPAL治療の解析を行った[14]．27例がALL，34例がAMLとしての治療を受け，5例が両者を組み合わせた治療を，1例がイマチニブ単独での治療を受けた(表5)．20例に自家移植あるいは同種移植が施行された．ALL治療が行われた27例中23例(85%)が完全寛解に到達した．これに対し，AML治療群で完全寛解に到達したのは34例中14例(41%)であり，15例は不応性で3例は早期に死亡した．また，ALLとAMLを組み合わせた治療を受けた5例のうち3例が寛解に到達したが，2例は感染症で死亡した．生存期間の検討では，全生存期間の中央値は18か月で，5年生存率は37%であり，治療別で見てみると，ALL治療群がその他の治療群に比べて有意に良好であった(図1)．予後因子解析では，成人，Ph染色体，AMLに準じた寛解導入療法が予後不良因子であった(表5)．以上の結果を踏まえると，成人やPh染色体陽性のMPALでは，第1寛解期での造血幹細胞移植を考慮すべきである．また，MPALの初回治療はALL治療に準じたレジメンが推奨されるものの，最終的な結論を得るためには大規模